



HAL
open science

Self-emulsifying drug delivery systems (SEDDS): how organic solvent release governs the fate of their cargo

Arne Matteo Jörgensen, Richard Wibel, Florina Veider, Barbara Hoyer, Joseph Chamieh, Herve Cottet, Andreas Bernkop-Schnürch

► To cite this version:

Arne Matteo Jörgensen, Richard Wibel, Florina Veider, Barbara Hoyer, Joseph Chamieh, et al.. Self-emulsifying drug delivery systems (SEDDS): how organic solvent release governs the fate of their cargo. International Journal of Pharmaceutics, 2023, 647, pp.123534. 10.1016/j.ijpharm.2023.123534 . hal-04624343

HAL Id: hal-04624343

<https://hal.umontpellier.fr/hal-04624343v1>

Submitted on 11 Dec 2024

HAL is a multi-disciplinary open access archive for the deposit and dissemination of scientific research documents, whether they are published or not. The documents may come from teaching and research institutions in France or abroad, or from public or private research centers.

L'archive ouverte pluridisciplinaire **HAL**, est destinée au dépôt et à la diffusion de documents scientifiques de niveau recherche, publiés ou non, émanant des établissements d'enseignement et de recherche français ou étrangers, des laboratoires publics ou privés.



Distributed under a Creative Commons Attribution 4.0 International License



Self-emulsifying drug delivery systems (SEDDS): How organic solvent release governs the fate of their cargo

Arne Matteo Jörgensen^a, Richard Wibel^a, Florina Veider^a, Barbara Hoyer^a, Joseph Chamieh^b, Hervé Cottet^b, Andreas Bernkop-Schnürch^{a,*}

^a Department of Pharmaceutical Technology, University of Innsbruck, Institute of Pharmacy, Center for Chemistry and Biomedicine, 6020 Innsbruck, Austria

^b IBMM, University of Montpellier, CNRS, ENSCM, 34095 Montpellier, France

ARTICLE INFO

Keywords:

Drug delivery
Drug release
Bioavailability
Nanoemulsions
Taylor dispersion analysis (TDA)
Diffusion coefficient

ABSTRACT

Organic solvents are commonly used in self-emulsifying drug delivery systems (SEDDS) to increase payloads of orally administered poorly soluble drugs. Since such solvents are released to a varying extent after emulsification, depending on their hydrophilic nature, they have a substantial impact on the cargo.

To investigate this impact in detail, quercetin and curcumin as model drugs were incorporated in SEDDS comprising organic solvents (SEDDS-solvent) of $\log P < 2$ and > 2 . SEDDS were characterized regarding size, payload, emulsification time and solvent release. The effect of solvent release on the solubility of these drugs was determined.

Preconcentrates of SEDDS-solvent $_{\log P < 2}$ emulsified more rapidly (< 1.5 min) forming smaller droplets than SEDDS-solvent $_{\log P > 2}$. Although, SEDDS-solvent $_{\log P < 2}$ preconcentrates provided higher quercetin solubility than the latter, a more pronounced solvent release caused a more rapid quercetin precipitation after emulsification (1.5 versus 4 h). In contrast, the more lipophilic curcumin was not affected by solvent release at all. Particularly, SEDDS-solvent $_{\log P < 2}$ preconcentrates provided high drug payloads without showing precipitation after emulsification.

According to these results, the fate of moderate lipophilic drugs such as quercetin is governed by the release of solvent, whereas more lipophilic drugs such as curcumin remain inside the oily phase of SEDDS even when the solvent is released.

1. Introduction

Up to date, poorly water-soluble drugs remain a major challenge for the pharmaceutical industry as these drugs face a complex combination of physicochemical, biological, physiological and anatomical factors that independently as well as collectively limit drug bioavailability (Boyd, 2019). Considering this multi-faceted challenge, self-emulsifying drug delivery systems (SEDDS) turned out to be a promising approach. The isotropic composition of oils, surfactants, co-surfactants and solvents provides relatively high solubility of drugs in the oily droplets during their transit through the gastrointestinal tract (Shah et al., 2014; Mohsin et al., 2009; Pouton, 2000). For many drugs, however, solubility in SEDDS is still not high enough resulting in insufficiently low payloads (Griesser et al., 2017). To improve drug solubility in SEDDS, various strategies including the formation of

hydrophobic ion pairs (Matteo Jörgensen, et al., 2022), the use of ionic liquids (Gamboa et al., 2020) as well as the addition of hydrophilic organic solvents are pursued (Shah et al., 2014) (Pouton, 2008). Hydrophilic solvents such as PEG400 ($\log P = -4.8$), dimethyl sulfoxide (DMSO) ($\log P = -1.35$), propylene glycol ($\log P = -0.9$) and ethanol ($\log P = -0.31$) are used to dissolve drugs in SEDDS preconcentrates and to raise the payload even in marketed products such as Neoral® (Novartis Pharmaceuticals Corporation, 2023), Aptivus® (Boehringer Ingelheim Pharmaceuticals, 2023) and Agenerase® (Glaxo Wellcome Inc, 2023). After emulsification of SEDDS preconcentrates in aqueous media, however, these hydrophilic solvents are immediately released from the oily droplets causing an unintended drug release and/or precipitation (Jörgensen et al., 2020). Consequently, the desired bioavailability enhancement is no longer provided.

In a recent study, we demonstrated that the less hydrophilic solvent

* Corresponding author at: Department of Pharmaceutical Technology, University of Innsbruck, Institute of Pharmacy, Center for Chemistry and Biomedicine, 6020 Innsbruck, Austria.

E-mail address: Andreas.Bernkop@uibk.ac.at (A. Bernkop-Schnürch).

<https://doi.org/10.1016/j.ijpharm.2023.123534>

Received 9 August 2023; Received in revised form 17 October 2023; Accepted 17 October 2023

Available online 18 October 2023

0378-5173/© 2023 The Author(s). Published by Elsevier B.V. This is an open access article under the CC BY license (<http://creativecommons.org/licenses/by/4.0/>).

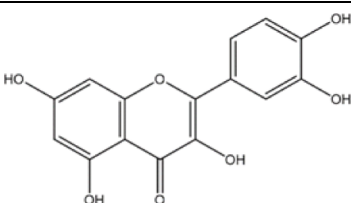
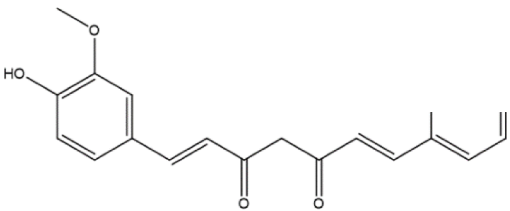
benzyl alcohol ($\log P = 1.1$), on the one hand, provides high solubilizing properties for poorly soluble drugs and, on the other hand, remains longer in the oily droplets (Jörgensen et al., 2020). So far, however, the fate of poorly soluble drugs during and after the release of more lipophilic solvents has not been investigated. It was therefore the aim of this study to evaluate the impact of more lipophilic solvents with $\log P$ values ranging from 1.2 to 3.97 on the fate of poorly soluble drugs in SEDDS. To the industrial relevance of this study, only FDA approved solvents were used (Food Additive Status List, 2022). More detailed information on solvents are provided in Table S-1. SEDDS with and without these solvents were developed, characterized, and evaluated regarding size, polydispersity index (PDI), ζ -potential and emulsification time. Subsequently, the release of solvents after emulsification was investigated using a semipermeable membrane as well as Taylor Dispersion Analysis (TDA). The fate of quercetin ($\log P = 1.5$) and curcumin ($\log P = 3.2$) (Table 1) serving as model drugs during the release of solvents was evaluated. In particular, drugs belonging to Biopharmaceutical Classification System (BCA) class II (quercetin) and IV (curcumin) exhibit characteristics that benefit from incorporation into SEDDS. Since the bioavailability of unformulated drugs within these classes is limited by their poor solubility as well as high (class II) or low (class IV) permeability through the intestinal mucosa.

2. Materials and methods

2.1. Materials

Cremonophor EL (polyethoxylated-35 castor oil = PEG35CO), quercetin (> 95 % HPLC, solid), curcumin (from *Curcuma longa* (Turmeric), powder), 2-phenylethanol (99 %), 2-phenoxyethanol (99 %), anhydrous anisole (99.7 %), citronellol (95 %), benzyl benzoate (99 %), eugenol (99 %) and ethanol (96 % v/v) were purchased from Sigma-Aldrich (Vienna, Austria). Capmul MCM C8 (glyceryl caprylate) was supplied by Abitec (Columbus, USA). Miglyol 812 (medium-chain triglyceride = MCT) was obtained by Caelo (Hilden, Germany). HPLC-grade solvents, acetonitrile and methanol were purchased from VWR (Linz, Austria). Lumogen F Red 305 (LR) was supplied by BASF (Ludwigshafen, Germany).

Table 1
Selection of model drugs.

Model drug	Structure	$\log P$	Water solubility [$\text{mg}\cdot\text{mL}^{-1}$]	BCS class	Ref.
Quercetin		1.5	0.06	II	(¹ National Center for Biotechnology Information. PubChem Compound Summary for CID 5, 2022) (Salehi, 2020)
Curcumin		3.2	0.003	IV	(¹ National Center for Biotechnology Information. PubChem Compound Summary for CID 969516, Curcumin. https://pubchem.ncbi.nlm.nih.gov/compound/969516 . Accessed Aug. 22, 2022) (Wang et al., 2017)

2.2. SEDDS development and characterization

2.2.1. Excipients screening and selection

The choice of suitable organic solvents was based on their lipophilicity to cover a broad $\log P$ range (Table 2). Benzyl alcohol served as reference solvent, since a complete release from SEDDS to the aqueous phase has already been shown previously (Jörgensen et al., 2020). Surfactants and oils are listed in Table 3.

2.2.2. Preparation of SEDDS preconcentrates

Two basic SEDDS preconcentrates (SEDDS-A and SEDDS-B) were developed for simple replacement of organic solvents while keeping the other ingredients as constant as feasible for comparison reasons. Briefly, 100 μL of SEDDS preconcentrates containing 20 % (v/v) of solvent, 45 % (v/v) of surfactant (PEG35CO) and 35 % (v/v) of oil were prepared by vortex mixing while heating with a heat gun at 60 °C (Table 4).

In each formulation, the ratio of the solvent and of the nonionic surfactant PEG35CO was kept constant. The prepared SEDDS preconcentrates can spontaneously emulsify upon contact with aqueous media under gentle agitation (Pouton, 2008). Traditionally, the formed dispersions are categorized into micro- and nanoemulsions based on their droplet size, which is highly dependent on the surfactant concentration (Pouton, 1997). Droplet sizes ranging between 100 and 250 nm are referred to microemulsions, whereas smaller sizes of less than 100 nm to nanoemulsions (Singh et al., 2012).

2.2.3. Selection and characterization of SEDDS

Mean droplet size, polydispersity index (PDI) and ζ -potential of each formulation were determined in demineralized water at 37 °C in a dilution rate of 1:100 by dynamic light scattering (DLS) utilizing Zetasizer Nano ZSP (Malvern Instruments, Worcestershire, UK) (Jörgensen et al., 2020). Subsequently, centrifugation and dissolution tests were conducted as previously described (Jörgensen et al., 2020) (Shafiq et al., 2007). Briefly, SEDDS were centrifuged 30 min at 800 g using a MiniSpin Centrifuge (Eppendorf, Hamburg, Germany) to evaluate the stability of the formed nanoemulsion. The self-emulsification times were assessed by adding 1 mL of SEDDS preconcentrate to 500 mL of demineralized water at 37 °C under gentle agitation at 50 rpm of the rotating

Table 2

Organic solvents for SEDDS development (Hansch, 1995; Verschueren, 1983; "National Center for Biotechnology Information, 2021; Yalkowsky, 2010; Valvani et al., 1981; "National Center for Biotechnology Information, 2021; "National Center for Biotechnology Information, 2021; "National Center for Biotechnology Information, 2021; "National Center for Biotechnology Information. PubChem Compound Summary for CID, 2345).

Organic solvent	Structure	LogP	Water solubility [mg·mL ⁻¹] at RT	Ref.
Solvent _{logP < 2}	Benzyl alcohol	1.1	35	[18][19]
	2-Phenoxy ethanol	1.16	26	[20][21]
	2-Phenyl ethanol	1.36	16	[18][22]
Solvent _{logP > 2}	Anisole/ methoxybenzene	2.11	1.04	[18][23]
	Eugenol	2.49	2.46	[21][24]
	Citronellol	3.2	0.2	[21][25]
	Benzyl benzoate	3.97	0.03	[18][26]

Table 3

Surfactant and oils used for SEDDS development.

Chemical name	Commercial name	Major compositions	HLB
PEG-35 castor oil (PEG35CO)	Cremonphor EL	Hydroxy C18:1 ^a	12–14
Glyceryl mono-/dicaprylate (glyceryl caprylate)	Capmul MCM C8	C8 Mono-/diesters	6–7 ^b
Medium chain triglyceride (MCT)	Miglyol 812	C8–C10 Triesters	15 ^c

^a value after the colon indicates the number of double bonds.

^b Reported by Abitec.

^c According to Macedo et al. (Macedo, et al., 2006).

Table 4

Composition of SEDDS pre-concentrate in % (v/v).

Component	Composition of pre-concentrate in % (v/v)	
	SEDDS-A	SEDDS-B
PEG35CO	45	45
Glyceryl caprylate	15	10
MCT	20	25
Organic solvent*	20*	

*listed in Table 2.

dissolution paddle of a standard USP XXII dissolution apparatus 2 (Erweka, Langen, Germany). The formation of emulsions was visually determined and evaluated by the grading system described previously (Shafiq et al., 2007).

2.3. Solvent release studies

2.3.1. Semipermeable membrane method

Solvent release from SEDDS droplets was evaluated in a two-compartment system. The compartments were separated by a dialysis membrane with cut off of 10–20 kDa (Carl Roth, Karlsruhe, Germany). In one compartment, 100 µL of SEDDS-solvent pre-concentrate was emulsified in demineralized water to a total volume of 1 mL and dialyzed against 2 mL of demineralized water at 37 °C. The opening of a 2 mL Eppendorf tube, which served as donor compartment, was sealed tightly using the dialysis membrane resulting in a membrane area of 0.79 cm². The donor compartment was subsequently submerged upside down in the acceptor compartment represented by a 50 mL falcon tube containing 2 mL of the release medium. The dialysis was conducted under shaking at 550 rpm on an Eppendorf ThermoMixer C (Hamburg, Germany) at 37 °C. At predetermined time points, aliquots of 100 µL were withdrawn from the release medium (2 mL of demineralized water) and replaced with 100 µL of fresh demineralized water. The concentration of solvent was quantified via HPLC as described below. The maximum concentration of solvent release was calculated and set to 100 %.

2.3.2. Quantification of organic solvents

The release of organic solvents was quantified using a Hitachi LaChrom Elite HPLC system (Tokyo, Japan) equipped with a L-2130 pump, a L-2200 autosampler, a L-2450 photodiode array UV detector and a Multo-High Bio 200 C18 column (250 × 4.6 mm, 5 µm). The mobile phase consisted of a binary solvent system of water/acetonitrile at 35 °C with an injection volume of 10 µL. The solvents were quantified following slightly modified methods described previously (Di Pietra et al., 1987; Villa et al., 2007; Reza et al., 2015; Foss, xxxx; Jakubíková et al., 2019). The optimized methods are summarized in Table 5.

Table 5
Liquid chromatographic methods for the determination of organic solvents.

Organic solvent	Mobile phase (ACN/H ₂ O v/v)	Flow rate (mL·min ⁻¹)	Detection (nm)	Ref.
Benzyl alcohol	60/40	1.2	258	(Di Pietra et al., 1987) (Villa et al., 2007)
Phenyl ethanol	60/40	1	258	(Reza et al., 2015)
Phenoxy ethanol	60/40	1	270	(Foss, xxxx)
Anisole	60/40	1	270	(Jakubíková et al., 2019)
Eugenol	60/40	1	280	(Villa et al., 2007)
Citronellol	70/30	1.2	220	(Villa et al., 2007)
Benzyl benzoate	60/40	1.8	231	(Villa et al., 2007)

2.3.3. Taylor dispersion analysis of solvent release

Taylor Dispersion Analysis (TDA) is an emerging technique based on the analysis of the dispersion of a solute plug, mobilized by pressure in a capillary tube under a laminar Poiseuille flow (Chamieh and Cottet, 2014; Cottet et al., 2007; Taylor, 1954; Taylor, 1953). By fitting experimental elution profiles with a Gauss function or sum of Gauss functions (Eq. (1)), one obtains the temporal peak variance (σ^2):

$$S(t) = \sum_{i=1}^n S_i(t) = \sum_{i=1}^n \frac{A_i}{\sigma_i \sqrt{2\pi}} e^{-\frac{1}{2} \frac{(t-t_0)^2}{\sigma_i^2}} \quad (1)$$

where $S(t)$ represents the experimental data points, t_0 is the average elution time of the solute (s), σ_i is the temporal variance corresponding to a species i (s), A_i is a concentration proportionality coefficient of the species i and depends on the response factor of each species at a specific detection wavelength.

From the obtained temporal variance, the molecular diffusion coefficient can be calculated using the simplified equation (Eq. (2)) (Cottet et al., 2014) (Cottet et al., 2007) and, consequently, the hydrodynamic diameter using the Stokes Einstein equation (Eq. (3)), respectively:

$$D = \frac{R_c^2 t_0}{24 \sigma^2} \quad (2)$$

$$D_h = \frac{k_b T}{3 \pi \eta D} \quad (3)$$

where R_c is the capillary radius (m), k_b is the Boltzmann constant (Pa m³/K), T is the analysis temperature (K), and η is the viscosity of the medium (Pa s). Eq. (2) is valid when the axial diffusion of the solute is negligible as compared to Taylor dispersion. More details about the conditions of validity are described elsewhere (Cottet et al., 2007; Ingram, 1954; Cottet et al., 2014).

TDA experiments were performed on an Agilent 7100 CE instrument (Waldbronn, Germany) using a 75 μ m internal diameter, fused silica capillary (Photon Lines, France), having a total length of 60 cm (51.5 cm to UV detector and 48 cm to LEDIF detector). The vial carousel was thermostated at 37 °C using an external circulating water bath Xtemp from Instrumat (Moirans, France). Between each analysis, capillaries were rinsed with the corresponding mobile phase (10 min). Samples were injected hydrodynamically (30 mbar, 4 s), on the inlet end of the capillary for the UV detection or on the outlet side for the LEDIF detection. The injected sample volume was kept at a value lower than 1 % of the capillary volume to the detector. Samples were mobilized with the corresponding mobile phase by applying a pressure of 50 mbar. The temperature of the capillary cartridge was set at 37 °C. The solutes were monitored using a UV DAD detector at 208 nm for phenyl ethanol and citronellol, at 235 nm for eugenol, at 254 nm for benzyl alcohol and

benzyl benzoate as well as at 270 nm for phenoxy ethanol and anisole. To determine the fate of the solvent, the capillary was filled with the formulation without solvent, followed by injecting a small plug of SEDDS containing the solvent. The plug was mobilized by the corresponding formulation without the solvent. To size the droplets of each formulation, Lumogen red (LR) was used as a hydrophobic fluorescent marker ($\log P = 17.46$). In the latter, the solutes were monitored by LEDIF fluorescence detection with an excitation at 480 nm, the emission light was collected through a ball lens and a high-pass filter in the wavelength range from 515 to 760 nm. In this case, the capillary was filled with the formulation containing the solvent, followed by injecting a plug of marked solvent with LR. This time, the plug was mobilized by the formulation containing the solvent. The Taylorgrams were recorded using Chemstation software and subsequently exported to Microsoft Excel for data processing.

2.4. Drug solubility studies

The maximum solubility of quercetin and curcumin in each SEDDS component as well as in final SEDDS preconcentrates was determined. For this purpose, an excess amount of the model drug was added to each component or to SEDDS preconcentrates, respectively, vortex mixed and kept on a thermomixer shaking at 2000 rpm at RT for 24 h. Afterwards, the samples were centrifuged for 15 min at 12,100 g. The concentration in saturated supernatants was examined via spectroscopy using a multimode microplate reader (TECAN Spark, Salzburg, Austria) according to slightly modified methods described previously (He et al., 2012) (Moussa et al., 2017). Quercetin was quantified by determining the absorbance of samples at a wavelength of 375 nm using EtOH as solvent. Curcumin concentrations of EtOH diluted samples were determined by fluorescence measurements using an excitation of 435 nm wavelength and an emission wavelength of 540 nm. The corresponding spectra are provided in Figure S-1. Based on these results, only SEDDS-solvent preconcentrates providing higher solubility than corresponding SEDDS preconcentrates without solvents were selected for further studies.

From the results of the solubility studies, the respective partition coefficient between the lipophilic phase (SEDDS) and the release medium (RM; demineralized water) was calculated. Additionally, the percentage of drug remaining inside SEDDS droplets (C_{SEDDS}) was calculated under the assumption of a dilution rate of 1:100 using Eq. (4), which is based on Nernst's distribution law:

$$C_{SEDDS}(\%) = \frac{100\%}{1 + \frac{V_{RM}}{V_{SEDDS} \times D_{SEDDS/RM}}} \quad (4)$$

where V_{RM} refers to the volume of release medium, V_{SEDDS} to the volume of SEDDS and $D_{SEDDS/RM}$ to the drug distribution between SEDDS and the release medium.

The equation assumes a drug release from SEDDS based on a simple diffusion process from a lipophilic liquid phase into an aqueous liquid phase. Thus, the only parameter controlling drug release is the distribution coefficient ($\log D$) that is calculated from the ratio of the drug solubility in SEDDS preconcentrate and in water (Bernkop-Schnürch and Jali, 2017).

2.5. Drug precipitation studies

Precipitation processes during solvent release were determined as described previously (Jørgensen et al., 2020). In brief, drug loaded SEDDS preconcentrates were dispersed in demineralized water at 37 °C (dilution ratio 1:100). Nanoemulsions were incubated on a thermomixer at 37 °C under shaking at 550 rpm. At predetermined time points, the samples were centrifuged at 12,100 g for 45 s to separate the precipitated drug from emulsions. The amount of drug remaining dissolved in the nanoemulsion was quantified via UV-Vis from aliquots of 20 μ L in

case of quercetin and or 10 μL of curcumin having been withdrawn from the supernatant. Demineralized water comprising the same amount of solvents (2 μL) served as control to exclude improved drug solubility in the aqueous phase due to solvent release.

2.6. Drug release monitored by TDA

Drug saturated SEDDS preconcentrates were prepared as described in section 2.4. After 24 h, preconcentrates were diluted 100-fold with demineralized water at 37 °C, vortexed and immediately placed in the capillary electrophoresis instrument's carousel at 37 °C for imminent injection to get the $t_{\text{incubation}} = 0$ h TDA data point. The TDA experimental setup was the same as described in section 2.3.3. The drug release was followed by UV detection at 375 nm for quercetin and 420 nm for curcumin for 24 h. The experimental peak area, proportional to the injected amount of soluble drug, was measured by peak integration and the average hydrodynamic diameter was calculated for each run as described in the previous TDA section. Each sample was mobilized by the corresponding formulation without the model drug in a dilution of 1:100. The individual hydrodynamic diameter was assessed by preparing a LR labelled formulation, which was mobilized with the unlabelled formulation. Furthermore, the hydrodynamic radii of free drugs in demineralized water were measured by TDA by injecting quercetin and curcumin solutions mobilized with demineralized water at 37 °C.

2.7. Statistical data analysis

When two sets of data were compared with each other, Student's *t*-test was applied. For the comparison of more than two data sets, one-way analysis of variance (ANOVA) and Bonferroni post hoc test were applied. GraphPad Prism 5 software was used for all statistical analyses.

3. Results and discussion

3.1. SEDDS development and characterization

SEDDS preconcentrates comprising 20 % of organic solvents, referred to as "solvents" in the following sections, were developed as listed in Table 2 based on our experience with similar formulations (Table 4). Comparability of formulations was provided by altering just the oily phase of SEDDS preconcentrates as slightly as necessary, depending on the solvent used (Table S-2). In total, nine formulations as

Table 6

Droplet size [nm] via DLS, hydrodynamic diameter $\langle D_h \rangle$ via TDA, PDI and ζ -potential [mV] of SEDDS preconcentrates dispersed in demineralized water (1:100) at 37 °C. Indicated values are means ($n \geq 3$) \pm SD.

Formulation	Droplet size [nm] (DLS)	$\langle D_h \rangle$ [nm] (TDA)	PDI (DLS)	ζ -Potential [mV]
SEDDS-A	19.35 \pm 0.36	25.09 \pm 1.24	0.06 \pm 0.01	-7.54 \pm 1.42
SEDDS-B	20.93 \pm 0.15	27.52 \pm 0.98	0.06 \pm 0.01	-7.25 \pm 0.81
SEDDS _{benzyl alcohol} ^(A)	23.84 \pm 0.77	22.16 \pm 0.58	0.04 \pm 0.01	-0.18 \pm 0.05
SEDDS _{phenoxy ethanol} ^(A)	25.10 \pm 0.40	26.56 \pm 0.28	0.37 \pm 0.05	-5.64 \pm 0.79
SEDDS _{phenyl ethanol} ^(B)	28.26 \pm 1.21	26.78 \pm 0.02	0.16 \pm 0.02	-4.32 \pm 1.32
SEDDS _{anisole} ^(A)	28.87 \pm 2.21	28.59 \pm 0.60	0.12 \pm 0.06	-3.93 \pm 0.36
SEDDS _{eugenol} ^(B)	33.53 \pm 1.61	37.28 \pm 1.00	0.06 \pm 0.03	-5.09 \pm 0.67
SEDDS _{citronellol} ^(A)	32.48 \pm 2.01	28.93 \pm 0.04	0.15 \pm 0.05	-4.23 \pm 0.12
SEDDS _{benzyl benzoate} ^(B)	36.99 \pm 1.60	35.79 \pm 0.28	0.08 \pm 0.02	-1.56 \pm 0.17

listed in Table 6 were tested. The capital letter in parentheses refers to the basic formulation and will not be used throughout the manuscript as no significant difference was observed in any of the studies in which the characteristics of SEDDS-A and SEDDS-B were compared ($p < 0.05$). Formulations were characterized regarding their size via DLS and TDA, PDI and ζ -potential. The comparatively small hydrodynamic diameter ranging from ~ 23 nm to ~ 37 nm can be attributed to the high amount of surfactant (45 % (v/v)) used in SEDDS preconcentrates (Thomas et al., May 2012). SEDDS comprising more hydrophilic solvents_{logP < 2} (SEDDS-solvent_{logP < 2}: benzyl alcohol, phenoxy ethanol or phenyl ethanol) tended to be smaller than formulations with more lipophilic solvents_{logP > 2} (SEDDS-solvent_{logP > 2}: anisole, eugenol, citronellol or benzyl benzoate). This suggests higher quantities of solvents might be present inside SEDDS droplets. The droplet size determined by DLS and the hydrodynamic diameter obtained by TDA are in broad agreement suggesting monodisperse nanoemulsions (Chamieh et al., 2015). Indeed, in the case of nanoemulsions where no marker is exchanged with the continuous phase, or in the case of slow exchange equilibria, TDA leads to a weight-average hydrodynamic diameter for a mass-sensitive detector, whereas DLS gives a harmonic z-average hydrodynamic diameter (Cottet et al., 2007). Thus, both methods will give the same average value for monodisperse samples. Furthermore, the relatively narrow polydispersity index (PDI) between 0.04 and 0.37 indicates the formation of monodisperse nanoemulsions by each formulation. Among them, however, SEDDS_{phenoxy ethanol} stands out with the highest PDI which is still considered acceptable.

The ζ -potential of SEDDS was slightly negative even though only non-charged excipients were used. This might be attributed to free fatty acids resulting from incomplete esterification of the glycerides or from degradation processes of fatty acid esters.

Furthermore, the self-emulsification time of each formulation was determined, indicating that SEDDS-solvent_{logP < 2} preconcentrates emulsified faster than corresponding formulations without solvent (Fig. 1).

On contrary, SEDDS-solvent_{logP > 2} preconcentrates needed a longer time to form homogeneous nanoemulsions. This observation, however, does not seem to correlate with the lipophilic character of solvents, as SEDDS_{citronellol} preconcentrate emulsified faster than the ones containing eugenol and anisole, although it has a higher logP. This result indicates that citronellol is more effective than eugenol and anisole, since self-emulsification does not only depend on surfactant, oil and the ratio of these two components, but also strongly on their interplay with the solvent (Jørgensen et al., 2020) (Rang and Miller, 1999). Only if a solvent is able to increase the flexibility of the hydrophobic tails of a water-soluble surfactant, it will lead to a faster dissolution and consequently shorter emulsification time of SEDDS preconcentrates (Pouton, 2008) (Date, 2008). Based on the obtained self-emulsification times and the appearance of formed nanoemulsions, SEDDS preconcentrates were classified into grades A-E (Table 7) as postulated by Shafiq et al. (Shafiq et al., 2007).

3.2. Release of solvents

3.2.1. Semipermeable membrane method

The release profiles of solvents are illustrated in Fig. 2. Within 6 h of incubation, less than 6 % of solvents_{logP > 2} were released from SEDDS-solvents_{logP > 2}. In contrast, the release profiles of benzyl alcohol, phenoxy ethanol and phenyl ethanol from SEDDS-solvents_{logP < 2} showed a nearly complete release over 6 h. It is well known that it generally takes around 6 h until equilibrium of small molecules is reached between two compartments that are separated from each other by the membrane used in this study (Waters et al., 2008). Therefore, the release of these hydrophilic solvents is presumably much faster than it can be monitored with a dialysis assay and a discrimination between the release controlling effect of SEDDS and of the separating membrane is almost impossible (Bernkop-Schnürch and Jalil, 2017).

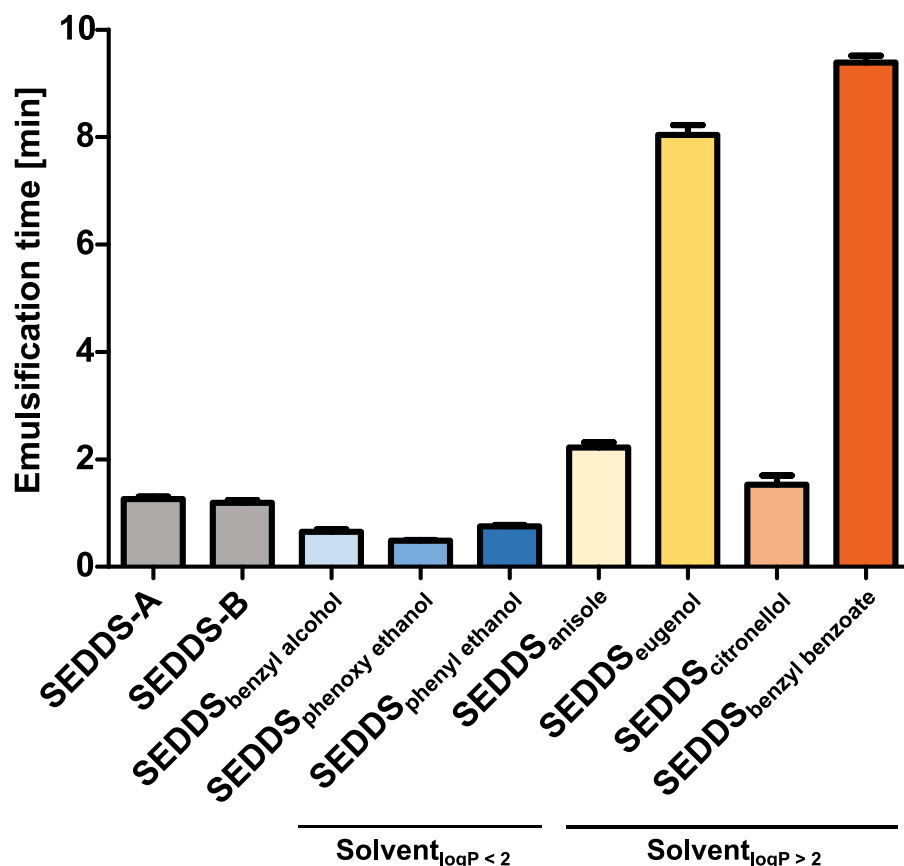


Fig. 1. Emulsification time of 1 mL of SEDDS preconcentrates without solvents (SEDDS-A, SEDDS-B) and with solvents in 500 mL of demineralized water at 37 °C under gentle agitation at 50 rpm of the rotation standard stainless-steel dissolution paddle. Indicated values are means ($n \geq 3$) \pm SD.

Table 7

Grade of nanoemulsions formed by SEDDS preconcentrates.

Grade	Nanoemulsion formation	Appearance	Formulation
A	< 1 min	Clear or bluish	SEDDS _{benzyl alcohol} SEDDS _{phenoxy ethanol} SEDDS _{phenyl ethanol}
B	> 1 min	Less clear, bluish white	SEDDS _{citronellol}
C	2 min	Fine milky	SEDDS _{anisole}
D	> 2 min	Dull, grayish white, slightly oily	SEDDS _{eugenol}
E	Poor/ minimal	Large oil globules on surface	SEDDS _{benzyl benzoate}

SEDDS-solvent_{logP < 2} preconcentrates consistently formed grade A nanoemulsions, whereas SEDDS-solvent_{logP > 2} ranged from B to E. These results demonstrate the essential role of solvents_{logP < 2} in the emulsification process as their higher supporting efficacy for surfactants resulted in a faster emulsification times.

To address these drawbacks, TDA was applied to provide stronger evidence for the release behavior of solvents obtaining results that are independent from the effect of the semipermeable membrane. It is important to note that sink conditions could not be provided for SEDDS-solvent_{logP > 2} due to poor water solubility of solvents.

3.2.2. Taylor dispersion analysis

Since Taylor Dispersion Analysis (TDA) is based on the analysis of the dispersion of a solute plug, mobilized by pressure in a capillary tube under a laminar Poiseuille flow it allows the determination of the molecular diffusion coefficient (D) of the solute, and subsequently its hydrodynamic diameter (D_h). The obtained experimental elution profile is

a Gaussian shaped peak (or sum of Gaussians) resulting from the combination of the parabolic velocity profile of the Poiseuille laminar flow and the molecular diffusion of the solutes (Chamieh and Cottet, 2014; Cottet et al., 2007; Taylor, 1954; Taylor, 1953).

Within the study, the diffusion of a “marker” (solvent or drug) in different formulations was traced by TDA. If the marker is 100 % liberated, the obtained size corresponds to the size of free marker in the continuous phase, i.e., water. If 100 % of the marker remains inside the droplet, the measured size corresponds to the droplet (measured independently by labeling the droplet with LR, $\log P = 17$). Fig. 3A shows the TDA elution profiles for formulations A and B omitting the solvents, while in Fig. 3B to 3H the light grey lines represent the elution profiles of the marker (LR) in formulations containing solvents. The size of each droplet obtained from these profiles is shown in Table 6.

Additionally, the size of each individual solvent was determined in demineralized water at 37 °C. The corresponding elution profiles are represented by the red dotted lines (Fig. 3A - H). These profiles were used to determine the D_h values ($D_{h,marker}$) of the free solvents (supporting information for D_h values, Figure S-4).

Finally, each formulation was analyzed by tracking the solvent at its specific UV wavelength. The Taylor dispersion of the obtained elution profiles (colored lines in Fig. 3B - 3H) is related to the average diffusion coefficient of the solvent, partitioned between droplet and continuous water phase (Jensen and Østergaard, 2010). Assuming that the response factor of the solvent is the same inside and outside of the droplet, the measured average diffusion coefficient is a weight average (Jensen and Østergaard, 2010) on the free solvent and on the droplet:

$$\langle D \rangle = D_{solvent}w_{free} + D_{droplet}(1 - w_{free}) \quad (5)$$

Consequently, the average hydrodynamic diameter $\langle D_h \rangle$ is a harmonic mean:

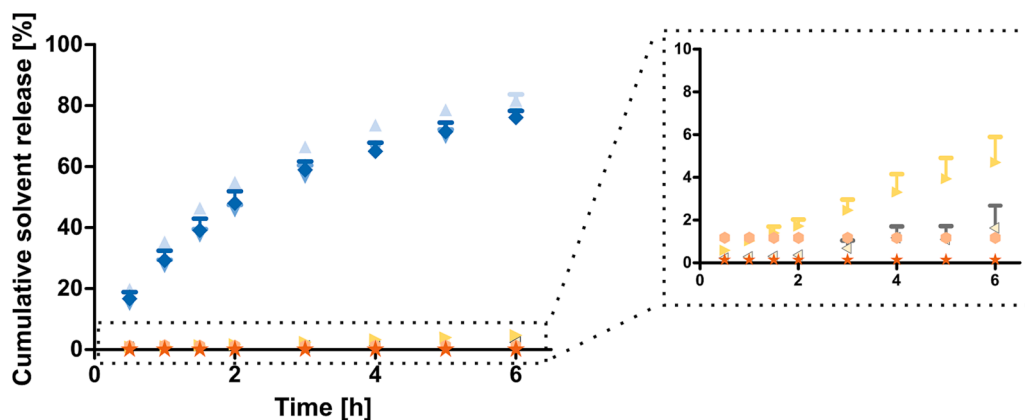


Fig. 2. Solvent release from SEDSS_{benzyl alcohol} (▲), SEDSS_{phenoxy ethanol} (▼), SEDSS_{phenyl ethanol} (◆), SEDSS_{anisole} (○), SEDSS_{eugenol} (►), SEDSS_{citronellol} (●), SEDSS_{benzyl benzoate} (★). 100 μ L of SEDSS were dissolved in demineralized water to a total volume of 1 mL and dialyzed against 2 mL of demineralized water at 37 °C under shaking at 550 rpm. Indicated values are means ($n \geq 3$) \pm SD.

$$\frac{1}{\langle D_h \rangle} = \frac{1}{D_{h,solvent}} w_{free} + \frac{1}{D_{h,droplet}} (1 - w_{free}) \quad (6)$$

and the free fraction of the solvent for each analysis can be calculated using the size of the droplet and of free solvent according to Eq. (7):

$$w_{free} = \frac{\left(\frac{1}{\langle D_h \rangle} - \frac{1}{D_{h,droplet}} \right)}{\left(\frac{1}{D_{h,solvent}} - \frac{1}{D_{h,droplet}} \right)} \quad (7)$$

Fig. 3I shows the resulting free fractions of solvents as a function of corresponding logP values. Each proportion was calculated at $t_{incubation} = 0$ h and 2 h. However, since no difference between these time points was observed, it is evident that the free proportion of solvent reached its partitioning equilibrium rapidly upon dispersion of the SEDSS preconcentrate in water. This result demonstrates a rapid partitioning of solvents between the droplet and the continuous phase without temporal progression. Consequently, this result provides evidence for a logP-dependent solvent release from SEDSS.

3.3. Impact of solvents on drug payload

The solubility study with quercetin and curcumin was conducted to evaluate the potential of drug solubilization for single components of SEDSS and final SEDSS preconcentrates. Initially, the solubilizing potential for the BCA class II drug quercetin was determined in single components and SEDSS preconcentrates. The achieved solubilities are shown in Fig. 4A and B.

Overall, solvents_{logP < 2} showed significantly higher solubility of quercetin than solvents_{logP > 2}. Nevertheless, the maximum solubility did not correlate strictly with the hydrophobicity of the solvents. Interestingly, the solubility in citronellol (> 15 mg·mL⁻¹) was significantly higher compared with anisole, eugenol and benzyl benzoate (< 5 mg·mL⁻¹). The maximum concentration in phenoxy ethanol and phenyl ethanol was > 2 -fold higher than in PEG35CO and in glyceryl caprylate (Fig. 4A). Quercetin was sparingly soluble in glyceryl caprylate and PEG35CO, which might be attributed to unesterified hydroxyl moieties (Date, 2008). In these components, quercetin was reaching even higher concentrations than in anisole, eugenol and benzyl benzoate.

This might be explained by the polar structure of the polyphenolic flavonoid quercetin exhibiting five hydroxyl moieties, which interact via hydrogen bonds with moderate to high polar solvents like benzyl alcohol, phenoxy ethanol and phenyl ethanol.

It is noteworthy that citronellol, as the only non-aromatic solvent, exhibits similar solubilizing properties for quercetin like benzyl alcohol and higher solubilization potential than eugenol. Likely, hydroxyl group

of citronellol interacts more efficiently with quercetin than the hydroxyl group of eugenol, which is probably hindered by intramolecular hydrogen bonds. The methoxy function of anisole as well as the ester moiety of benzyl benzoate provide solely weak hydrogen bond acceptor properties as the valence electrons are engaged in the aromatic systems. Overall, these findings are in good agreement with previous studies (Seal, 2016) (Ghasemzadeh et al., 2011).

Fig. 4B shows the resulting payloads in SEDSS preconcentrates. Due to the addition of solvents, the solubility of quercetin in SEDSS preconcentrates was 2- to 3-fold higher. Merely the addition of anisole did not follow this trend. Solvents_{logP < 2} showed the highest impact on increasing drug payloads in SEDSS preconcentrates. In contrast, the addition of solvents_{logP > 2} led to lower drug concentrations, which is in agreement with the drug solubility in single solvents (Fig. 4A).

Based on the drug solubility in SEDSS preconcentrates and in water (release medium; RM), the distribution coefficient ($\log D_{SEDSS/RM}$) was determined for each SEDSS-solvent (Fig. 4C). Formulations with $\log D$ values above the corresponding SEDSS without solvent (SEDSS-A and SEDSS-B) were selected for further drug precipitation studies. Therefore, SEDSS_{anisole} was excluded as no beneficial solubilizing properties were provided for quercetin.

Since drug release from SEDSS was shown to be controlled by the $\log D$ between the lipophilic phase (SEDSS) and the release medium such as the intestinal fluid or saliva, the percentage of drug remaining inside the SEDSS droplets was calculated from these data according to Nernst's distribution law (Fig. 4D) (Bernkop-Schnürch and Jalil, 2017). According to these calculations, a remaining drug amount of ≥ 82 % up to 91 % inside the droplets after emulsification is anticipated. However, since solvent release from SEDSS might affect drug solubility in the release medium and thus the drug distribution, these ratios might be decreased.

Similarly, the curcumin (BCS class IV) solubilizing properties of each solvent and of SEDSS preconcentrates containing them was evaluated. According to its logP of 3.2, the drug should predominantly remain in the oily phase of SEDSS (Ramshankar et al., 2008). Results confirmed that SEDSS-solvent_{logP < 2} preconcentrates reaching drug concentrations > 20 mg·mL⁻¹ were superior in comparison to SEDSS-solvent_{logP > 2} preconcentrates (Fig. 5A). Among them, eugenol provided the highest curcumin payload. The lowest solubilizing potential of solvents showed citronellol followed by benzyl benzoate and anisole. In case of oils/surfactant the following rank order was observed: PEG35CO $>$ glyceryl caprylate $>$ MCT.

According to these results, substances with the ability to form hydrogen bonds, on the one hand, combined with the ability of interacting via van der Waals or π -stacking forces, on the other hand, solubilize curcumin effectively, which is in good agreement with a previous

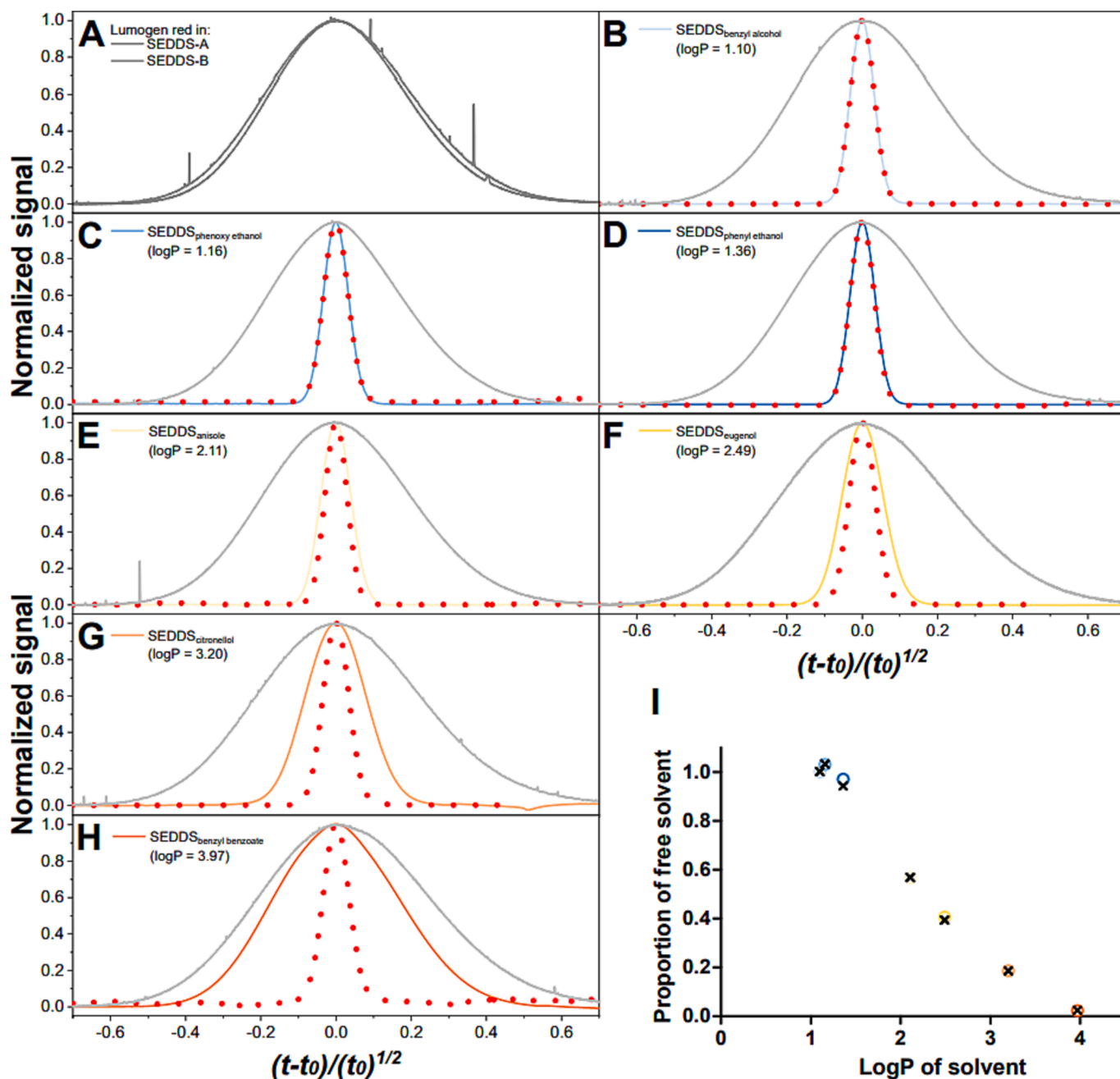


Fig. 3. (A - H) Taylorgrams of pure solvents in demineralized water (red dots), formulated solvents in SEDDS (colored line) detected by UV, LR marked SEDDS (A grey lines; B to H light grey line) detected by LEDIF. (I) Proportion of free solvent directly after emulsification (○) and after 2 h (×) of incubation at 37 °C. (For interpretation of the references to colour in this figure legend, the reader is referred to the web version of this article.)

study (Bergonzi et al., 2014).

In comparison with quercetin, the subsequent solubility study in SEDDS preconcentrates (Fig. 5B) demonstrated a more pronounced effect of solvents_{logP < 2}.

The preconcentrates of SEDDS_{benzyl alcohol}, SEDDS_{phenoxy ethanol}, SEDDS_{phenyl ethanol} and SEDDS_{anisole} provided a 2- to 8-fold enhancement in payload compared to the corresponding SEDDS preconcentrate without the solvent. Especially benzyl alcohol, phenyl ethanol and anisole were able to increase the solubility of curcumin in SEDDS preconcentrates. The most outstanding result in this regard is apparently the co-solvency effect of anisole when it was added to the formulation. The payload strongly increased in SEDDS_{anisole} preconcentrates in comparison to the solubility of curcumin in single excipients. Preliminary solubility studies in single solvents might be thus misleading

due to co-solvency or anti-solvency effects occurring in final mixtures (Solanki et al., 2013; Shi et al., 2021; Uquiche et al., 2016).

The preconcentrates of SEDDS_{anisole} and SEDDS-solvent_{logP < 2} showed a 5- to 10-fold increase in $D_{\text{SEDDS}/\text{Water}}$ (Fig. 5C) compared to the corresponding SEDDS preconcentrates without the solvents. In contrast, SEDDS_{benzyl benzoate} preconcentrate exhibited just a minor increase and preconcentrates of SEDDS_{eugenol} as well as SEDDS_{citronellol} showed no solubility enhancement at all. Thus, the latter two formulations were excluded from drug precipitation studies. The predicted percentage of curcumin remaining inside the droplets was for all SEDDS-solvents ≥ 94 % (Fig. 5D).

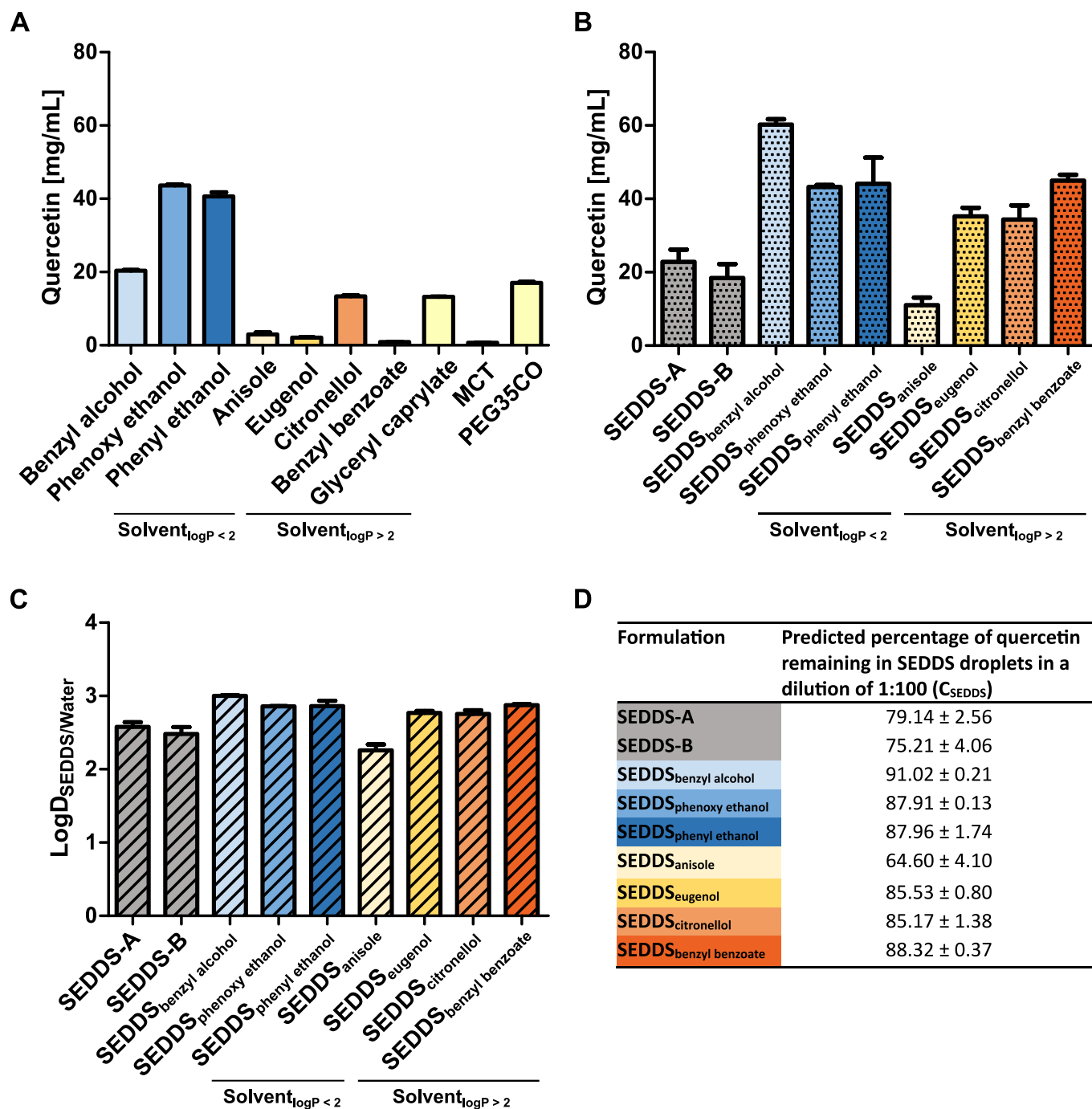


Fig. 4. (A) Maximum solubility of quercetin in solvents, oils, and surfactant; (B) maximum solubility of quercetin in SEDDS preconcentrates; (C) distribution coefficient ($\log D$) of SEDDS preconcentrates and water for quercetin; (D) predicted percentage of quercetin remaining in SEDDS droplets after emulsification of SEDDS preconcentrate. Indicated values are means ($n \geq 3$) \pm SD.

3.4. Precipitation studies

3.4.1. Quercetin precipitation from SEDDS

Quercetin saturated SEDDS_{solvent} preconcentrates were emulsified in demineralized water to form nanoemulsions of varying quercetin concentrations relative to their payload.

The formed nanoemulsions initially showed stable quercetin concentrations until the drug started to precipitate in the aqueous phase after 1.5 h of incubation from SEDDS_{benzyl alcohol}, SEDDS_{phenoxy ethanol}, SEDDS_{phenyl ethanol} (Fig. 6A) and SEDDS_{eugenol} (Fig. 6B).

The precipitation continued reaching 40 to 60 % within 6 h.

SEDDS_{benzyl benzoate} showed the fastest onset of precipitation but subsequently remained at a precipitation of around 25 %. The corresponding SEDDS without a solvent did not show any precipitation at all (Figure S-2) providing evidence for a solvent release dependent effect. Controls at concentrations of 0.2 % (v/v) of solvent in demineralized water, which is equivalent to an entire solvent release, did not affect solubility under the same conditions (Table S-3). Thus, improved solubility of quercetin in the aqueous phase due to released solvents can be excluded.

The precipitation of quercetin from SEDDS can be explained by solvent release. Due to this release, drug solubility in SEDDS droplets is not provided anymore resulting in a time-dependent precipitation

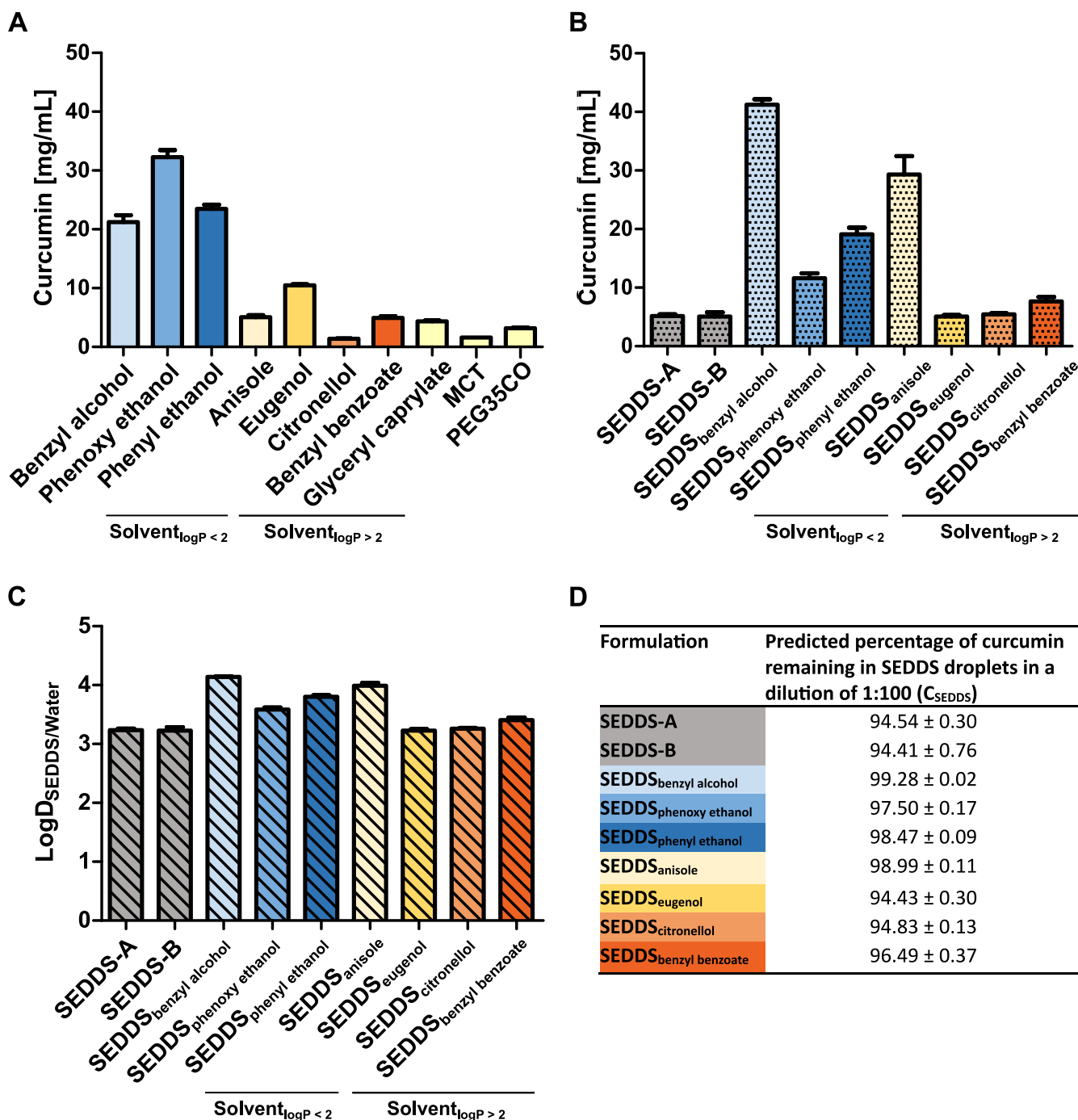


Fig. 5. (A) Maximum solubility of curcumin in solvents, oils and surfactant; (B) maximum solubility of curcumin in SEDDS preconcentrates; (C) distribution coefficient ($\log D$) of SEDDS preconcentrates and water for curcumin; (D) predicted percentage of quercetin remaining in SEDDS droplets after emulsification of SEDDS preconcentrate. Indicated values are means ($n \geq 3$) \pm SD.

process. As citronellol remains predominantly inside the oily droplets ($\geq 80\%$ as quantified previously by TDA), its solubilizing capacity for quercetin can be maintained for a longer period.

To evaluate whether higher drug concentrations are still provided in nanoemulsions, the initial drug concentration of SEDDS preconcentrates was compared with the final drug concentration of formed nanoemulsions after incubation for 6 h at 37 °C (Fig. 7).

After 6 h of incubation, solely for SEDDS_{eugenol} a significant difference ($* = P \leq 0.05$) between SEDDS comprising a solvent and corresponding SEDDS without the solvent was observed. This can be explained by the release of solvent, which carries the drug to the surface

of the SEDDS droplet triggering drug precipitation at the interphase between SEDDS droplet and aqueous phase. The precipitation continues until the drug concentration in the nanoemulsion reaches the drug concentration of the corresponding SEDDS without the solvent. Nevertheless, drug loss due to precipitation could be protracted for 1.5 to 4 h providing a prolonged time for drug absorption (Fig. 6).

The solubilization state should ideally be provided throughout the small intestinal transit time to achieve improved intestinal absorption (Augustijns and Brewster, 2012). To further prolong or even prevent drug loss, precipitation inhibitors can be applied (Xua, xxxx). Moreover, bioavailability might benefit from an amorphous precipitation state as

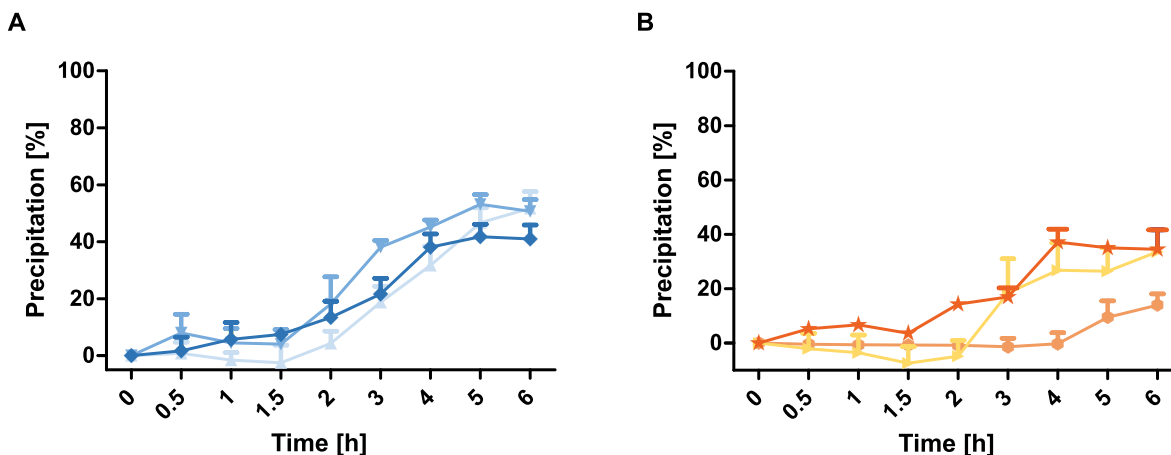


Fig. 6. Precipitation of quercetin from SEDDS emulsified in demineralized water (1:100) within 6 h at 37 °C while shaking at 550 rpm on a thermomixer. (A) SEDDS-solvent_{logP} < 2: SEDDS_{benzyl alcohol} (▲), SEDDS_{phenoxy ethanol} (▼) and SEDDS_{phenyl ethanol} (◆). (B) SEDDS-solvent_{logP} > 2: SEDDS_{eugenol} (►), SEDDS_{citronellol} (●) and SEDDS_{benzyl benzoate} (★). Indicated values are means (n ≥ 3) ± SD.

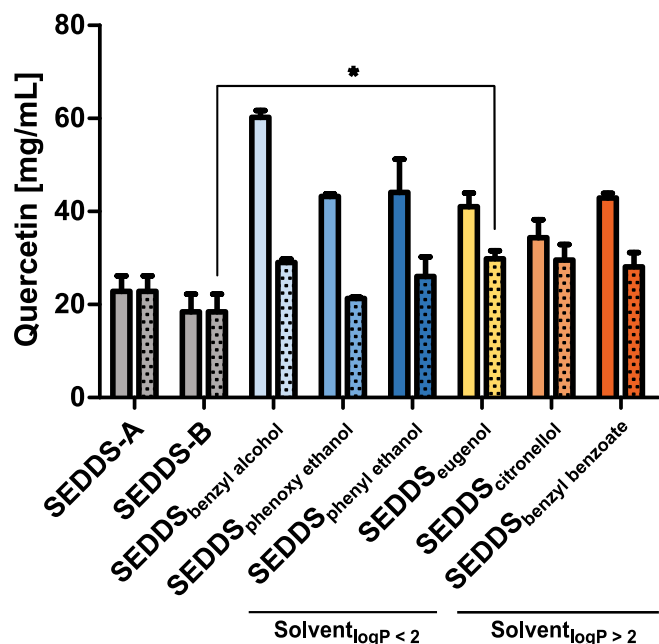


Fig. 7. Quercetin concentration in SEDDS droplets after 0 h (columns without filling) and after 6 h of incubation (dotted columns) in demineralized water in a ratio of 1:100 while shaking at 550 rpm on a thermomixer (37 °C). Indicated values are means (n ≥ 3) ± SD.

long as the drug is not prone to instability in body fluids, since the loss of the advantages associated with the carrier system such as protection from hydrolysis and from enzymatic degradation must be considered (Jörgensen et al., 2020).

3.4.2. Curcumin precipitation from SEDDS

The precipitation-time profiles of curcumin loaded SEDDS showed no drug precipitation for at least 6 h due to the addition of solvents (data not shown). Enhanced curcumin solubility in the aqueous phase due to released solvents could be excluded, since 0.2 % (v/v) of solvent dissolved in demineralized water, which is equivalent to a complete solvent release, showed a negligible improvement under the same experimental conditions (Table S-2).

Although, solvents_{logP} < 2 rapidly diffuse from SEDDS to the aqueous medium, the provided drug concentrations remained stable without

precipitation in the presence of formed nanoemulsions. This observation might be explained by the comparatively higher logP of curcumin keeping it to a higher extent in the oily phase.

3.4.3. Drug release monitored via TDA

Drug release from SEDDS in demineralized water (1:100), was monitored by TDA as the obtained peak area of each run is proportional to the soluble fraction of the drug (Fig. 8A and 9A).

Fig. 8 was divided in two parts according to the logP of the used solvent. The initial peak area of SEDDS-solvent_{logP} < 2 was higher in comparison with corresponding SEDDS-A and SEDDS-B at $t_{incubation} = 0$ h. Over time, the peak area decreased due to drug release until reaching a plateau after ~ 4 h of incubation corresponding to the value that is obtained for SEDDS-A and SEDDS-B. This indicates that the solvent has no effect on the final equilibrium. SEDDS-solvent_{logP} > 2 reached the final plateau later. SEDDS comprising eugenol and benzyl benzoate required ~ 6–8 h to reach the equilibrium.

The free soluble proportion of quercetin as obtained from TDA runs decreased in all cases to reach the values obtained with the formulations without solvents (Fig. 8). This implies that when the equilibrium is reached, only bulk water and the oily droplet are governing the partitioning of the drug in SEDDS and the solvent has little or no effect on the final equilibrium. Due to the progressive drug precipitation after the release from the droplet, the free drug proportion decreased from an average value of 5 % to about 2.5 % (Fig. 8B). These results are in good agreement with the solubility data presented in Figs. 6 and 7.

In the case of curcumin (Fig. 9A), the peak area remained constant throughout 24 h of incubation at 37 °C in all cases indicating no release of the drug. This absence of precipitation agrees with the respective studies (Fig. 9). The partitioning equilibrium was reached immediately at the first instances of incubation and the free proportions varied only between 0 and 1 % (Fig. 9B).

Finally, the full potential of TDA was used to determine the free soluble proportion of the drug as well as the proportion remaining inside the droplets allowing to calculate a logD value at each analyzed point. The D_h values for each formulation at all injection times are provided in Figure S-4. The values of logD_{SEDDS/RM} were obtained for each TDA run by using the calculated proportions in a dilution ratio of 1:100. These values did not increase with incubation time, suggesting that the logD_{SEDDS/RM} of the drug is the dominating parameter, controlling its release from the droplet within the initial dispersion (Figure S-5).

The use of solvents increased the payload in droplets. When the saturated SEDDS preconcentrates are dispersed in the RM, two phenomena can occur. Firstly, upon formation of the droplets the solvent is partitioned between the droplets and the RM and since it is responsible

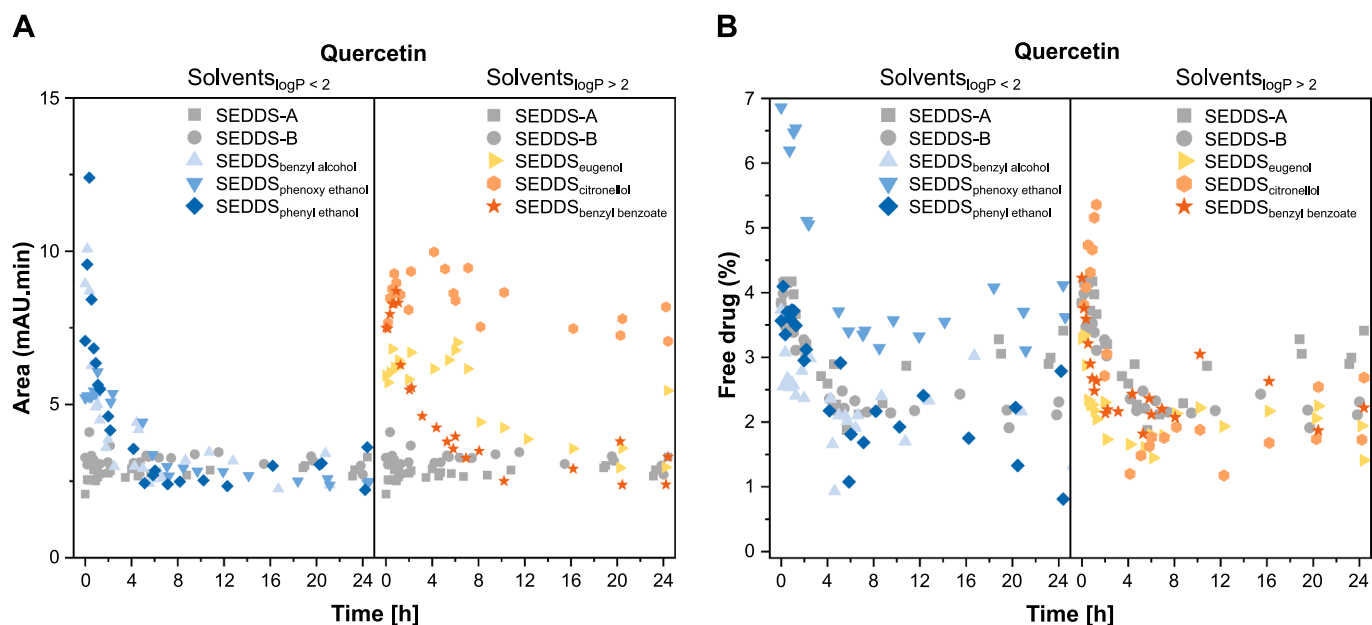


Fig. 8. Evolution of (A) peak area and (B) proportion of free soluble quercetin, calculated using Eq. (7), with incubation time followed for 24 h for all studied SEDDS.

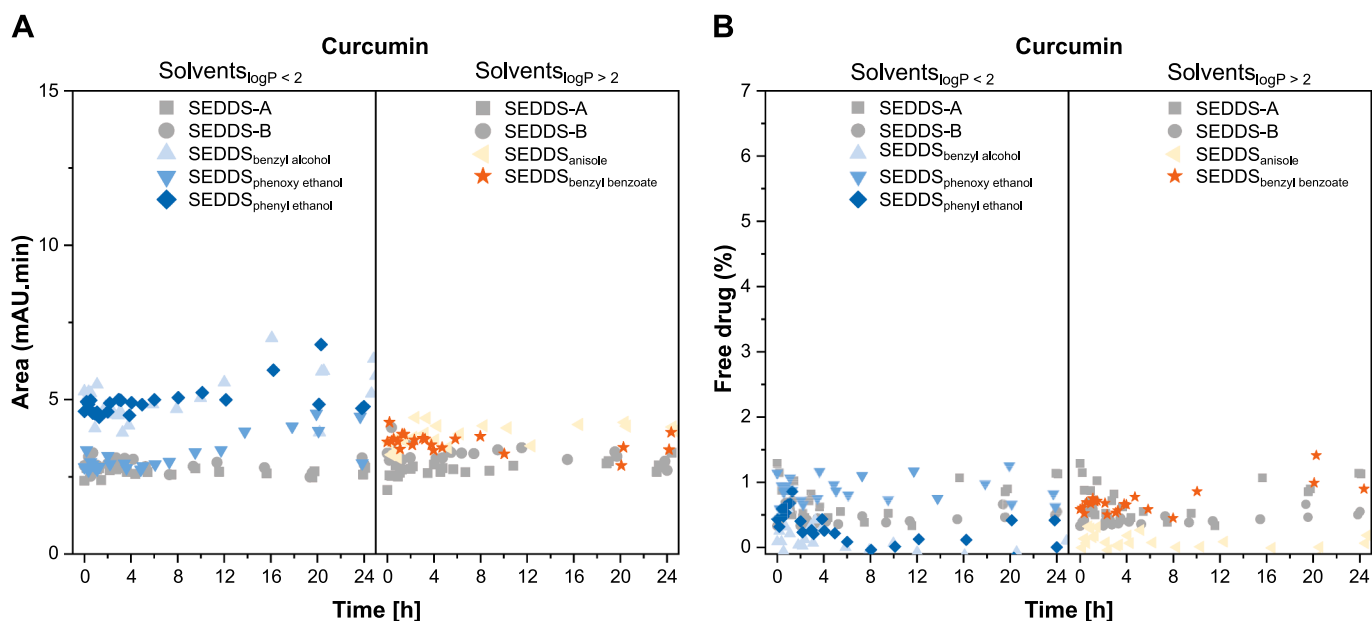


Fig. 9. Evolution of (A) area evolution and (B) proportion of free soluble curcumin, calculated using Eq. (7), with incubation time followed for 24 h for all studied SEDDS.

for the drug solubility it might drag the drug with it to the surface of SEDDS droplets. Secondly, the drug is partitioned between the RM and the droplet. In this case, the drug concentration in the RM exceeds the drug solubility, precipitation occurs (Figure S-6) resulting in a decreased concentration in the RM and thus decreased TDA peak areas. Subsequently, this precipitation shifts the partitioning equilibrium toward a continuous drug release from the droplets until reaching the equilibrium of maximum solubility in the RM and inside the droplets. At this point, no further precipitation occurs as the drug is partitioned according to its $\log D_{\text{SEDDS}/\text{RM}}$ value between the droplet and RM.

4. Conclusion

Numerous marketed SEDDS such as Neoral® (Novartis

Pharmaceuticals Corporation, 2023), Aptivus® (Boehringer Ingelheim Pharmaceuticals, 2023) and Agenerase® (Glaxo Wellcome Inc, 2023) contain the hydrophilic solvents ethanol, propylene glycol or PEG400. These solvents, however, are rapidly released from the oily droplets formed during the emulsification process (Jörgensen et al., 2020). This solvent release have a substantial impact on the fate of incorporated lipophilic drugs in SEDDS. In order to investigate this complex process, TDA was introduced as highly potent alternative method to well-established methods such as dialysis. It enables the monitoring of release and precipitation processes during and after solvent release without any delays. The obtained results within this study showed that the fate of the quercetin was essentially affected by the release of hydrophilic solvents resulting in unintended precipitation of cargo which occurred 1.5 – 4 h after emulsification. Among tested solvents, the more

lipophilic solvents (solvents_{logP} > 2) turned out to be advantageous providing enhanced drug solubilization for a longer period of time. In particular, citronellol (logP = 3.2) guaranteed a fast emulsification of SEDDS preconcentrate (< 2 min) while remaining inside SEDDS droplets by ≥ 80 % for 6 h. In contrast, benzyl alcohol (logP = 1.1) having been identified as the most suitable solvent so far remained just by 0–20 % in SEDDS under the same conditions (Jörgensen et al., 2020). The fate of the more lipophilic curcumin, however, was independent from solvent release. In this case, more hydrophilic solvents (solvents_{logP} < 2) providing rapid emulsification and high drug solubility in SEDDS preconcentrates can be used.

Taken all, solvents have a fundamental impact on the efficacy of SEDDS containing moderate lipophilic drugs. Formulators will have to find the best compromise between solubility enhancement and risk of premature drug release and precipitation. Based on the findings of this study, the efficacy of most SEDDS containing moderate lipophilic cargos might be improved.

List of chemical compounds.

Anisole anhydrous (99.7 %)
Capmul MCM C8 (glyceryl caprylate)
Curcumin (from <i>Curcuma longa</i> (Turmeric), powder)
Benzyl benzoate (99 %)
Citronellol (95 %)
Cremophor EL (polyethoxylated-35 castor oil = PEG35CO)
Eugenol (99 %)
Quercetin (> 95 % HPLC, solid)
2-phenoxyethanol (99 %)
2-phenylethanol (99 %)

CRediT authorship contribution statement

Arne Matteo Jörgensen: Conceptualization, Methodology, Investigation, Visualization, Writing – original draft. **Richard Wibel:** Methodology, Investigation. **Florina Veider:** Investigation. **Barbara Hoyer:** Investigation. **Joseph Chamieh:** Conceptualization, Methodology, Investigation, Writing – original draft. **Hervé Cottet:** Conceptualization, Supervision, Funding acquisition. **Andreas Bernkop-Schnürch:** Conceptualization, Writing – review & editing, Supervision, Funding acquisition.

Declaration of Competing Interest

The authors declare that they have no known competing financial interests or personal relationships that could have appeared to influence the work reported in this paper.

Data availability

Data will be made available on request.

Acknowledgements

The Centre for International Cooperation and Mobility (ICM) of the Austrian Agency for Education and Internationalisation (OeAD-GmbH) has selected this project for support (Project No FR 13/2020). The financial support was provided by the Federal Ministry of Education, Science and Research (BMBWF). The authors would like to acknowledge this support as well as the support of the French Ministry of Foreign Affairs (MAEE) and the French Ministry for Higher Education and Research (MESR) (Project PHC AMADEUS 2020 N°44090VA). A. M. Jörgensen received a doctoral scholarship for the promotion of young researchers at the Leopold-Franzens-University Innsbruck.

Appendix A. Supplementary data

Supplementary data to this article can be found online at <https://doi.org/10.1016/j.ijpharm.2023.123534>.

References

- “National Center for Biotechnology Information (2021). PubChem Compound Summary for CID 8842, Citronellol. Retrieved August 19, 2021 from <https://pubchem.ncbi.nlm.nih.gov/compound/3,7-dimethyloct-6-en-1-ol>.”
- “National Center for Biotechnology Information (2021). PubChem Compound Summary for CID 3314, Eugenol. Retrieved August 19, 2021 from <https://pubchem.ncbi.nlm.nih.gov/compound/Eugenol>.”
- “National Center for Biotechnology Information (2021). PubChem Compound Summary for CID 7519, Anisole. Retrieved August 19, 2021 from <https://pubchem.ncbi.nlm.nih.gov/compound/Anisole>.”
- “National Center for Biotechnology Information (2021). PubChem Compound Summary for CID 31236, 2-Phenoxyethanol. Retrieved August 19, 2021 from <https://pubchem.ncbi.nlm.nih.gov/compound/2-Phenoxyethanol>.”
- “National Center for Biotechnology Information. PubChem Compound Summary for CID 2345, Benzyl benzoate’ PubChem, <https://pubchem.ncbi.nlm.nih.gov/compound/Benzyl-benzoate>. Accessed 19 August, 2021.”
- “National Center for Biotechnology Information. PubChem Compound Summary for CID 5280343, Quercetin. <https://pubchem.ncbi.nlm.nih.gov/compound/quercetin#section=Melting-Point>. Accessed Aug. 22, 2022.”
- “National Center for Biotechnology Information. PubChem Compound Summary for CID 969516, Curcumin. <https://pubchem.ncbi.nlm.nih.gov/compound/969516>. Accessed Aug. 22, 2022.”
- Augustjns, P., Brewster, M.E., 2012. Supersaturating drug delivery systems: Fast is not necessarily good enough. *J. Pharm. Sci.* 101 (1), 7–9.
- Bergonzi, M.C., Hamdouch, R., Mazzacava, F., Isacchi, B., Bilia, A.R., 2014. Optimization, characterization and invitro evaluation of curcumin microemulsions. *LWT - Food Sci. Technol.* 59 (1), 148–155.
- Bernkop-Schnürch, A., Jalil, A., 2018. “Do drug release studies from SEDDS make any sense?,” *J. Control. Release* 271 (October 2017), 55–59.
- Boehringer Ingelheim Pharmaceuticals, “Aptivus [prescribing information],” *U.S. Food and Drug Administration*. [Online]. Available: https://www.accessdata.fda.gov/drugsatfda_docs/label/2011/021814s0111bl.pdf. [Accessed: 17-May-2023].
- Boyd, B.J., et al., 2019. Successful oral delivery of poorly water-soluble drugs both depends on the intraluminal behavior of drugs and of appropriate advanced drug delivery systems. *Eur. J. Pharm. Sci.* 137.
- Chamieh, J., Cottet, H., 2014. “Size-based characterisation of nanomaterials by Taylor dispersion analysis,” *Colloid Interface Sci. Pharm. Res. Dev.* 173–192.
- Chamieh, J., Davanier, F., Jannin, V., Demarne, F., Cottet, H., 2015. Size characterization of commercial micelles and microemulsions by Taylor dispersion analysis. *Int. J. Pharm.* 492 (1–2), 46–54.
- Cottet, H., Biron, J.P., Martin, M., 2007. Taylor dispersion analysis of mixtures. *Anal. Chem.* 79 (23), 9066–9073.
- Cottet, H., Martin, M., Papillaud, A., Souaïd, E., Collet, H., Commeyras, A., 2007. Determination of dendrigraft poly-L-lysine diffusion coefficients by Taylor dispersion analysis. *Biomacromolecules* 8 (10), 3235–3243.
- Cottet, H., Biron, J.P., Martin, M., 2014. On the optimization of operating conditions for Taylor dispersion analysis of mixtures. *Analyst* 139 (14), 3552–3562.
- Date, A.A., Nagarsenker, M.S., 2008. “Parenteral microemulsions: An overview,” *Int. J. Pharm.* 355 (1–2), 19–30.
- Di Pietra, A.M., Cavrini, V., Raggi, M.A., 1987. Determination of benzaldehyde traces in benzyl alcohol by liquid chromatography (HPLC) and derivative UV spectrophotometry. *Int. J. Pharm.* 35 (1–2), 13–20.
- “Food Additive Status List | FDA.” [Online]. Available: <https://www.fda.gov/food/food-additives-petitions/food-additive-status-list>. [Accessed: 05-Aug-2022].
- J. Foss, “Analysis of Common Preservatives in Personal Care Products by HPLC with UV Detection,” pp. 1–7.
- Gamboa, A., Schüßler, N., Soto-Bustamante, E., Romero-Hasler, P., Meinel, L., Morales, J. O., 2020. Delivery of ionizable hydrophilic drugs based on pharmaceutical formulation of ion pairs and ionic liquids. *Eur. J. Pharm. Biopharm.* 156, 203–218.
- Ghasemzadeh, A., Jaafar, H.Z.E., Rahmat, A., 2011. Effects of solvent type on phenolics and flavonoids content and antioxidant activities in two varieties of young ginger (*Zingiber officinale* Roscoe) extracts. *J. Med. Plants Res.* 5 (7), 1147–1154.
- Glaxo Wellcome Inc, “Agenerase [product information],” *U.S. Food and Drug Administration*. [Online]. Available: https://www.accessdata.fda.gov/drugsatfda_docs/label/2002/21007s11,21039s101bl.pdf. [Accessed: 17-May-2023].
- Griesser, J., Hetényi, G., Moser, M., Demarne, F., Jannin, V., Bernkop-Schnürch, A., 2017. Hydrophobic ion pairing: Key to highly payloaded self-emulsifying peptide drug delivery systems. *Int. J. Pharm.*
- Hansch, D.H., Leo, C., Hoekman, A., 1995. Exploring QSAR: Hydrophobic, electronic, and steric constants. *Am. Chem. Soc.*
- He, Y., He, Z., He, F., Wan, H., 2012. “Determination of quercetin plumbagin and total flavonoids in *Drosera peltata* Smith var. *glabrata* Y.Z.Ruan”. *Pharmacogn. Mag* 8 (32), 263.
- Ingram, T.G., 1954. Conditions under which dispersion of a solute in a stream of solvent can be used to measure molecular diffusion. *Proc. R. Soc. Lond.* A225473–477.
- Jakubíková, M., Sáděcká, J., Hroboňová, K., 2019. Classification of plum brandies based on phenol and anisole compounds using HPLC. *Eur. Food Res. Technol.* 245 (8), 1709–1717.

- Jensen, H., Østergaard, J., 2010. Flow induced dispersion analysis quantifies noncovalent interactions in nanoliter samples. *J. Am. Chem. Soc.* 132 (12), 4070–4071.
- Jörgensen, A.M., Friedl, J.D., Wibel, R., Chamieh, J., Cottet, H., Bernkop-Schnürch, A., 2020. Cosolvents in self-emulsifying drug delivery systems (SEDDS): Do they really solve our solubility problems? *Mol. Pharm.* 17 (9), 3236–3245.
- Macedo, J.P.F., et al., 2006. "Micro-emultocrit technique: A valuable tool for determination of critical HLB value of emulsions". *AAPS PharmSciTech* 7 (1), E146–E152.
- Matteo Jörgensen, A., et al., 2022. "Biodegradable arginine based steroid-surfactants: Cationic green agents for hydrophobic ion-pairing". *Int. J. Pharm.* 122438.
- Mohsin, K., Long, M.A., Pouton, C.W., 2009. Design of lipid-based formulations for oral administration of poorly water-soluble drugs: Precipitation of drug after dispersion of formulations in aqueous solution. *J. Pharm. Sci.* 98 (10), 3582–3595.
- Moussa, Z., Chebl, M., Patra, D., 2017. Fluorescence of tautomeric forms of curcumin in different pH and biosurfactant rhamnolipids systems: Application towards on-off ratiometric fluorescence temperature sensing. *J. Photochem. Photobiol. B Biol.* 173, 307–317.
- Novartis Pharmaceuticals Corporation, "Neoral Soft Gelatin Capsules Neoral Oral Solution [prescribing Information]," *U.S. Food and Drug Administration website*. [Online]. Available: https://www.accessdata.fda.gov/drugsatfda_docs/label/2009/050715s027,050716s0281bl.pdf. [Accessed: 17-May-2023].
- Pouton, C.W., 1997. Formulation of self-emulsifying drug delivery systems. *Adv. Drug Deliv. Rev.*
- Pouton, C.W., 2008. Formulation of lipid-based delivery systems for oral administration: Materials, methods and strategies. *Adv. Drug Deliv. Rev.* 60 (6), 625–637.
- C.W. Pouton "Lipid formulations for oral administration of drugs: non-emulsifying self-emulsifying and 'self-microemulsifying' drug delivery systems" 2000.
- Ramshankar, Y.V., Suresh, S., Devi, K., 2008. Novel self-emulsifying formulation of curcumin with improved dissolution, antiangiogenic and anti-inflammatory activity. *Clin. Res. Regul. Aff.* 25 (4), 213–234.
- Rang, M.J., Miller, C.A., 1999. Spontaneous emulsification of oils containing hydrocarbon, nonionic surfactant, and oleyl alcohol. *J. Colloid Interface Sci.* 209 (1), 179–192.
- Reza, H., Fereshteh, N., Saman, A.N., 2015. Determination of phenylethyl alcohol by reversed-phase high-performance liquid chromatography (RP-HPLC) in Budesonide nasal spray. *African J. Pure Appl. Chem.* 9 (5), 81–90.
- Salehi, B., et al., 2020. Therapeutic potential of quercetin: New insights and perspectives for human health. *ACS Omega* 5 (20), 11849–11872.
- Seal, T., 2016. Quantitative HPLC analysis of phenolic acids, flavonoids and ascorbic acid in four different solvent extracts of two wild edible leaves, *Sonchus arvensis* and *Oenanthe linearis* of North-Eastern region in India. *J. Appl. Pharm. Sci.* 6 (2), 157–166.
- Shafiq, S., Shakeel, F., Talegaonkar, S., Ahmad, F.J., Khar, R.K., Ali, M., 2007. Development and bioavailability assessment of ramipril nanoemulsion formulation. *Eur. J. Pharm. Biopharm.* 66 (2), 227–243.
- Shah, S.M., Jain, A.S., Kaushik, R., Nagarsenker, M.S., Nerurkar, M.J., 2014. Preclinical formulations: Insight, strategies, and practical considerations. *AAPS PharmSciTech* 15 (5), 1307–1323.
- Shi, H., Xie, Y., Xu, J., Zhu, J., Wang, C., Wang, H., 2021. Solubility enhancement, solvent effect and thermodynamic analysis of pazopanib in co-solvent mixtures. *J. Chem. Thermodyn.* 155, 106343.
- Singh, B., Bandopadhyay, S., Kapil, R., Singh, R., parkash katara, O., 2012. Self-emulsifying drug delivery systems (SEDDS): Formulation development, characterization, and applications. *Crit. Rev. Ther. Drug Carr. Syst.* 26 (5), 427–451.
- Solanki, S.S., Soni, L.K., Maheshwari, R.K., 2013. Study on mixed solvency concept in formulation development of aqueous injection of poorly water soluble drug. *J. Pharm.* 2013, 1–8.
- Taylor, G.I., 1953. Dispersion of soluble matter in solvent flowing slowly through a tube. *Proc. R. Soc. London. Ser. A. Math. Phys. Sci.* 219 (1137), 186–203.
- Taylor, G.I., 1954. The dispersion of matter in turbulent flow through a pipe. *Proc. R. Soc. London. Ser. A. Math. Phys. Sci.* 223 (1155), 446–468.
- Thomas, N., Müllertz, A., Graf, A., Rades, T., 2012. Influence of lipid composition and drug load on the in vitro performance of self-nanoemulsifying drug delivery systems. *J. Pharm. Sci.* 101 (5), 1721–1731.
- Uquiche, E., Antilaf, I., Millao, S., 2016. Enhancement of pigment extraction from *B. braunii* pretreated using CO₂ rapid depressurization. *Brazilian J. Microbiol.* 47 (2), 497–505.
- Valvani, S.C., Yalkowsky, S.H., Roseman, T.J., 1981. Solubility and partitioning IV: Aqueous solubility and octanol-water partition coefficients of liquid nonelectrolytes. *J. Pharm. Sci.* 70 (5), 502–507.
- Verschuere, K., 1983. *Handbook of environmental data on organic chemicals*, 2nd ed. Van Nostrand Reinhold, New York, NY.
- Villa, C., Gambaro, R., Mariani, E., Dorato, S., 2007. High-performance liquid chromatographic method for the simultaneous determination of 24 fragrance allergens to study scented products. *J. Pharm. Biomed. Anal.* 44 (3), 755–762.
- Wang, Y., Wang, C., Zhao, J., Ding, Y., Li, L., 2017. A cost-effective method to prepare curcumin nanosuspensions with enhanced oral bioavailability. *J. Colloid Interface Sci.* 485, 91–98.
- Waters, N.J., Jones, R., Williams, G., Sohal, B., 2008. Validation of a rapid equilibrium dialysis approach for the measurement of plasma protein binding. *J. Pharm. Sci.* 97 (10), 4586–4595.
- S. Xua W.G. Dai "Drug precipitation inhibitors in supersaturable formulations" *International Journal of Pharmaceutics* 453 1 Elsevier B.V., 2013 36 43.
- P. Yalkowsky S.H. He Yan Jain *Handbook of Aqueous Solubility Data Second Edition*. CRC Press Boca Raton 2010.